IEEE Photonics Journal
An IEEE Photonics Society Publication

Gate-Free InGaAs/InP Single-Photon Detector Working at Up to 100 Mcount/s

Volume 5, Number 4, August 2013

Alberto Tosi
Carmelo Scarcella
Gianluca Boso
Fabio Acerbi

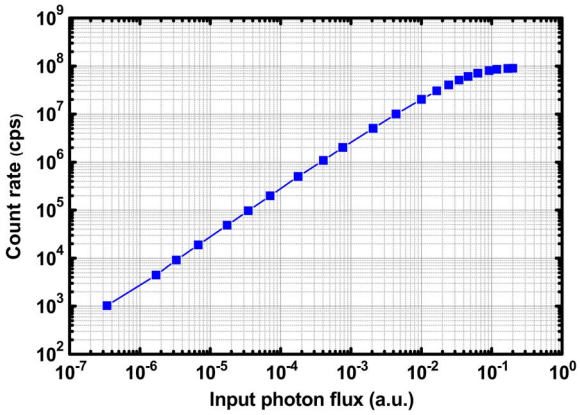

DOI: 10.1109/JPHOT.2013.2278526
1943-0655 © 2013 IEEE

Gate-Free InGaAs/InP Single-Photon Detector Working at Up to 100 Mcount/s

Alberto Tosi, Carmelo Scarcella, Gianluca Boso, and Fabio Acerbi

Dipartimento di Elettronica, Informazione e Bioingegneria, Politecnico di Milano, 20133 Milano, Italy

DOI: 10.1109/JPHOT.2013.2278526

Manuscript received July 18, 2013; revised August 8, 2013; accepted August 8, 2013. Date of publication August 15, 2013; date of current version August 27, 2013. Corresponding author: A. Tosi (e-mail: alberto.tosi@polimi.it).

Abstract: Recently, there has been considerable effort to develop photon-counting detectors for the near-infrared wavelength range, but the main limitation is to have a practical detector with both high count rates and low noise. Here, we show a novel technique to operate InGaAs/InP single-photon avalanche diodes (SPADs) in a free-running equivalent mode at high count rate up to 100 Mcount/s. The photodetector is enabled with a 915-MHz sinusoidal gate signal that is kept unlocked with respect to the light stimulus, resulting in a free-running equivalent operation of the SPAD, with an afterpulsing probability below 0.3%, a photon detection efficiency value of 3% at 1550 nm, a temporal resolution of 150 ps, and a dark count rate below 2000 count/s. Such gate-free approach can be used to measure, at high count rate, signals in continuous wave or with slow time decays, where standard gated detectors would not be suitable.

Index Terms: Photodetectors, single-photon avalanche diodes, photon counting, near-infrared detector, avalanche photodiode.

1. Introduction

Single photon detectors are required in a wide variety of applications in the near-infrared (NIR) wavelength range, between 1.0 and 1.7 μm, where very fast and faint signals must be detected. Such applications include quantum cryptography (Quantum Key Distribution, QKD), Optical Time Domain Reflectometry (OTDR), eye-safe laser ranging (Light Detection And Ranging, LIDAR), VLSI circuit characterization based on light emission from hot carriers in MOSFETs, singlet oxygen detection for dosimetry in PhotoDynamic Therapy (PDT), time-resolved spectroscopy, etc.

Many of these applications require a free-running detector able to operate at high count rates (tens to hundreds of Mcount/s). In quantum cryptography, for example, fiber-based (working at 1550 nm) and free space (typically at 1064 nm) QKD systems need high-count-rate detectors to guarantee high secret-bit rates [1]. The ideal detector should also work in free-running mode in order to avoid issues related to the synchronization between the transmitter and the receiver, which can lead to strong reduction of the system detection efficiency [2], and to prevent its vulnerability to illumination attacks [3]. Other applications could also benefit from non-gated detectors, like LIDAR with gigahertz clock rates [4] and singlet oxygen detection, where long time constants need to be reconstructed [5].

Current solutions, adopted by many research laboratories, are based on Superconducting Single-Photon Detectors (SSPD) [6]. Such detectors withstand high count rates and are operated in free-running mode, but need to be cooled at cryogenic temperature, forcing to use bulky cryostats that impair their applicability at a larger scale.

A valuable alternative to SSPDs is the use of Single-Photon Avalanche Diodes (SPADs). They are low-power and reliable microelectronic photodetectors that fully exploit carrier multiplication when

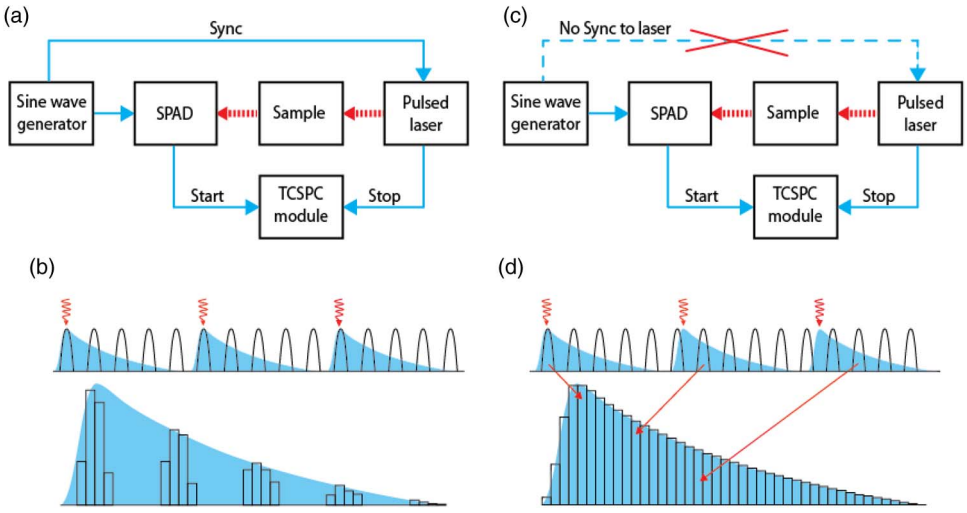

Fig. 1. Working principle of the gate-free technique. a) Typical sinusoidal gating setup where a SPAD is enabled with a sinusoidal signal that is synchronized to the laser stimulus. b) Sampling of the optical signal by the sine gated SPAD. c) Gate-free setup where the SPAD detector has a completely independent synchronization source. d) Waveforms showing an unlocked SPAD detector sampling at different time intervals the optical signal, resulting in a free-running equivalent mode.

biased above their breakdown voltage: when a single photon is absorbed, it triggers a self-sustaining avalanche, easily detectable by the read-out circuitry [7].

SPADs sensitive in the near-infrared wavelength range (up to 1.7 μm) are fabricated with low bandgap semiconductor materials, such as Ge and InGaAs. Devices with InGaAs absorption region and InP multiplication region proved to have the best performance [8], but must be generally used in gated-mode, where the detector is turned ON (above its breakdown voltage) only for a short period of time (few nanoseconds) followed by a long hold-off period (up to few tens of microseconds) where the detector is kept in the OFF state [9]. This technique is used to limit afterpulsing, which is almost proportional to the charge flown during an avalanche [8].

To overcome the intrinsic low throughput of the standard gating technique due to its long hold-off time, different fast-gating methods have been developed, some based on sub-nanosecond square-wave gate signals [10], while others based on gigahertz sine wave gating [11]–[14]. These techniques allow to use InGaAs/InP SPADs at high count rates thanks to a strong reduction of the afterpulsing probability and hence of the required hold-off time, but are suitable only for periodic optical signals with a short duration ($<$ 1 ns) because of their limited ON time.

Recently a SPAD with integrated passive quenching resistor has been developed to allow free-running operation of InGaAs/InP SPADs by reducing the avalanche charge [15] thanks to faster passive avalanche quenching, but in this case the throughput is limited to below 1 Mcount/s.

In this paper we present a novel technique for InGaAs/InP SPADs based on gigahertz sinusoidal gating that accomplishes an equivalent free-running operation of the detector while withstanding a remarkable throughput of 100 Mcount/s. A state-of-the-art InGaAs/InP SPAD is sine-gated at a frequency of 915 MHz to reduce the charge flow per avalanche while the gate signal is kept unlocked from the light pulses to be measured. Relying on the asynchronous behavior of the detector with respect to the signal to be acquired, optical waveforms can be reconstructed without ON time limitation, like in any free-running detector.

2. Free-Running Equivalent Principle

Fig. 1 shows a comparison between the standard sine-gating technique and the proposed free-running equivalent mode that we called "*gate-free*" mode.

In a typical sine-gated setup [Fig. 1(a)], the photodetector is turned ON and OFF by a sinusoidally modulated bias voltage at a frequency ranging from few hundred megahertz to above one

gigahertz. The optical waveform to be reconstructed is typically a pulse with a clock frequency derived from the same synchronization signal used for the photodetector, or vice versa. Since many commercial laser systems work at repetition frequency below 100 MHz, the trigger signal to ignite laser emission is usually a divide-by-N version of the gigahertz gating signal of the photodetector. This signal is also used as the time base for the Time-Correlated Single-Photon Counting (TCSPC) board that collects the photon arrival times.

Since sinusoidal gating relies on very short ON times (less than 1 ns) to reduce the afterpulsing probability by reducing the avalanche charge, the gate signal must be accurately delayed in time to match the arrival time of the photons on to the detector. The laser pulse is hence synchronized with the peak of the sinusoidal bias in order to achieve the best performance in terms of photon detection efficiency (PDE) and timing jitter [Fig. 1(b)]. While this technique is effective where short and periodic light signals have to be detected (e.g. Quantum Key Distribution, QKD), many applications require to reconstruct long decay constants (e.g. time-resolved spectroscopy of highly diffusing media) or non-periodic photon arrival times (e.g. CW single-photon sources).

If we unlock the detector gate from the trigger signal of the light source [Fig. 1(c)], photons from the optical waveform can hit the detector in any possible bias state [Fig. 1(d)] resulting in a flat response in time of the detector. In other words, the gate does not "select" a specific portion of the optical waveform since the detector gate is not synchronized with it. To explain this, let's consider two sine waves, the first is that of the SPAD gate and second is at the frequency of the repetition rate of the optical signal to be measured. The two sine waves are not locked and are at two independent frequencies f_1 (SPAD gate) and f_2 (signal rate). Since the SPAD is ON only during the positive half wave, the detector will sample the signal at different times every period $T_1 = 1/f_1$, again because the two waves are not in phase. Additionally, the phase noise of the two waves will introduce a time jitter that randomizes the sampling pattern. The result is that, after many periods T_1, the SPAD is sampling uniformly the optical signal to be reconstructed, hence the mean behavior is equivalent to the free-running mode, where the detector is always ON except for a hold-off time: the SPAD is in the OFF state for a certain amount of time but since this state is not synchronized with the optical stimulus, some photons are just randomly discarded while the others are collected without a dependence on their arrival time. Compared to a real free-running detector, the gate-free one has the advantage of a very low afterpulsing probability due to the extremely short ON time (less than 500 ps). This enables very high count rate in applications where it was not possible with standard techniques.

3. Experimental Setup

Fig. 2(a) shows the block diagram of the experimental setup used to characterize the behavior of an InGaAs/InP SPAD with the gate-free technique. The SPAD is a bare die wire-bonded to a custom passive-quenching front-end board in order to minimize parasitic effects. The board has been mounted into a vacuum chamber and cooled to 220 K with a four-stage thermo-electric cooler (the minimum achievable temperature is 190 K).

The sinusoidal signal for the SPAD gate at 915 MHz is derived from a commercial sine-wave generator and later amplified (25 dB) by a chain of two RF power amplifiers. To preserve the spectral purity of the signal a Surface Acoustic Wave (SAW) band-pass filter (BPF) is placed between the output of the last power amplifier and the SPAD front-end board. The SAW filter has been chosen because it minimizes dimensions and results in a very pure sine wave due to its narrow pass-band (26 MHz) and high off-band rejection ratio ($>$ 40 dB).

The SPAD front-end includes a ballast resistor R_Q for passive quenching and a capacitor C_P for AC coupling the avalanche signal to the following circuit, both connected at the SPAD anode. The gate is applied to the SPAD cathode, where resistor R_T is used for impedance matching.

The typical signal after the coupling capacitor is the result of a small avalanche signal ($<$ 1 mV) and a strong sinusoidal disturbance ($>$ 1 V) caused by the capacitive feed-through of the gate signal. There are many different techniques in literature to suppress the sinusoidal signal [11]–[14]. We implemented a hybrid solution comprising a first self-differencing circuit with a wide-bandwidth ($>$ 4 GHz) balun transformer and a custom-made microstrip notch filter [16].

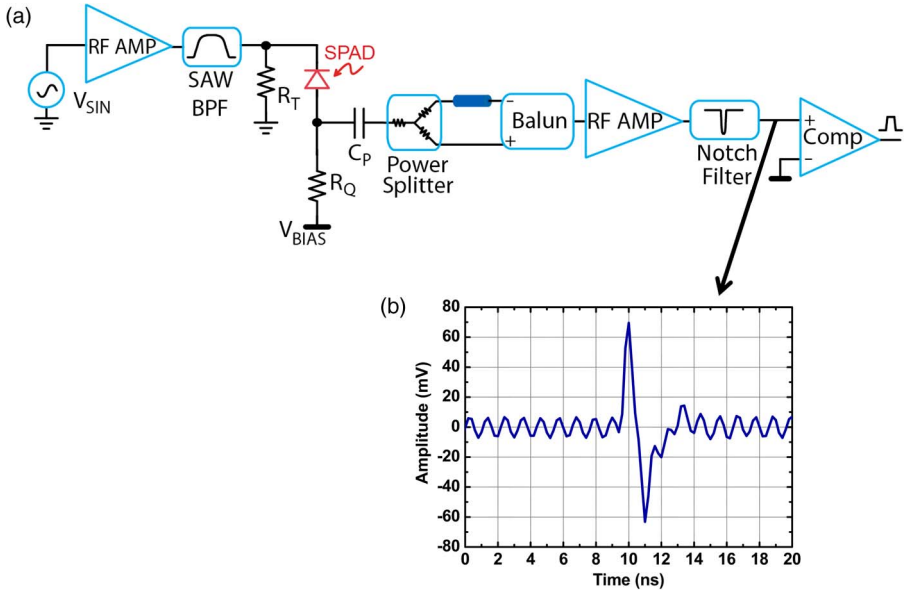

Fig. 2. Experimental setup. a) Block diagram of the experimental setup used to demonstrate the gate-free mode for InGaAs/InP SPADs. b) Avalanche read-out signal acquired after the RF amplifiers for a sinusoidal gate peak amplitude of 7 V at 915 MHz. Both the avalanche signal and the spurious capacitive coupling of the gate are clearly visible.

Two RF low-noise amplifiers are placed between the balun and the notch filter to amplify the avalanche signal by 40 dB and improve the overall impedance matching of the detection chain. The resulting signal [see Fig. 2(b)] is fed to a fast comparator to extract a digital pulse synchronous with the photon arrival time. The comparator includes a monostable, so that the output pulse lasts 10 ns, thus implementing a count-off time of 10 ns: once an avalanche pulse is sensed, successive pulses are masked for 10 ns in order to avoid spurious clicks due to spikes and oscillations in the detected signal.

4. Measurements

In order to test the performance of the free-gated setup, we employed an InGaAs/InP SPAD developed at Politecnico di Milano [17]. The detector active area has a diameter of 25 μm. The SPAD has been wire-bonded to our custom front-end board and cooled to 220 K. The detector is biased with a DC voltage of 63.45 V corresponding to its breakdown voltage at 220 K. A sinusoidal voltage at 915 MHz is AC coupled to the SPAD cathode and its peak amplitude has been swept from 3 V to 7 V, which corresponds to the maximum excess bias V_{EX} of the present setup.

The system has been characterized in terms of photon detection efficiency, dark count rate, timing resolution, afterpulsing probability and linearity of the count rate. To demonstrate the improvement of the gate-free technique, the same SPAD has also been operated in standard square-gating mode at similar conditions for comparison.

4.1. Photon Detection Efficiency

In order to evaluate the photon detection efficiency (PDE) of the InGaAs/InP SPAD under test we employed a calibrated optical test bench consisting of a light-tight compartment, a calibrated broadband white light lamp, a monochromator, an integrating sphere and a set of optical filters. The filters, the monochromator and the integrating sphere are used to select from the white spectrum of the lamp a specific wavelength and to shine on the detector a controlled photon flux. The efficiency of the system is therefore calculated from the ratio between the photons impinging on the SPAD active area and the acquired SPAD counts.

We measured the photon detection efficiency of the system for both the sinusoidal gate-free and the classical square-wave gating in a range between 800 nm and 1650 nm, at steps of 25 nm. Fig. 3(a)

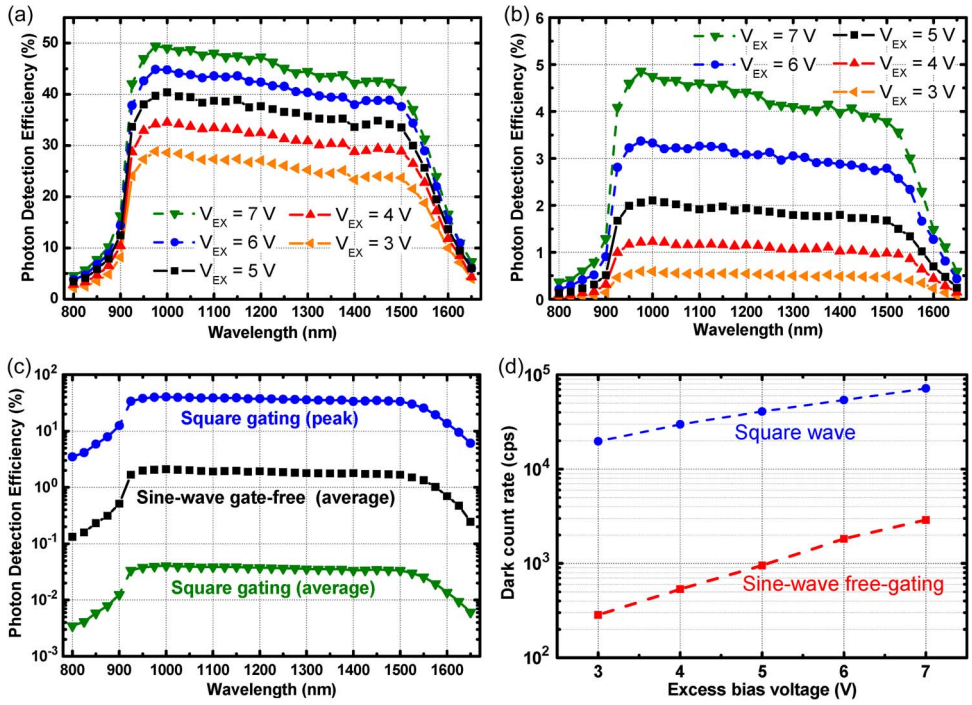

Fig. 3. Photon detection efficiency and noise of the gate-free system. a) and b) Photon detection efficiency measured at wavelengths between 800 nm and 1650 nm for an InGaAs/InP SPAD gated with different techniques and with peak excess bias voltages ranging from 3 V to 7 V. a) Peak PDE measured during $T_{ON} = 100$ ns with a square-wave gate signal at $f_{GATE} = 10$ kHz. b) Average PDE measured with a sine-wave gate signal at 915 MHz. c) PDE comparison with different gating schemes at $V_{EX} = 5$ V: while the square-wave technique features PDE > 40% during the ON time, its limited duty cycle (1/1000 in this example) is a disadvantage for non-periodic signals where the average efficiency have to be considered. d) Dark count rate dependence on excess bias voltage at 220 K for the same InGaAs/InP SPAD gated with two different techniques. The circles represent the DCR measured with a standard square-wave gating, while the squares represent the DCR measured with a sine-wave gate-free approach.

shows the PDE measured when gating the detector with a square wave signal at $f_{GATE} = 10$ kHz ($T_{GATE} = 100\ \mu$s) with an ON time of $T_{ON} = 100$ ns. The results are then normalized by the duty cycle to obtain the efficiency during the ON time, thus obtaining a peak efficiency of 50% at $V_{EX} = 7$ V. Fig. 3(b) shows the PDE obtained with the gate-free configuration where the SPAD is gated by a sinusoidal wave at 915 MHz and the efficiency is averaged by the intrinsic continuous shifts between ON and OFF states of the detector. The peak efficiency at $V_{EX} = 7$ V is 5%, while it is still above 3% at 1550 nm. Fig. 3(c) shows a comparison at $V_{EX} = 5$ V between the two methods: the detection efficiency decreases by a factor of 10 when operated in gate-free (squares) compared to the efficiency obtained during the ON time of a square-wave gating (circles). However, if the optical signal to be measured is non-periodic (e.g. CW signals), the effective PDE of the square-wave gating is much less, e.g. T_{GATE}/T_{ON} times lower (i.e. 100 μs/100 ns = 1000 times lower for this example) than the gate-free one (triangles) when CW signals are acquired, due to the low duty cycle that it is needed to keep the afterpulsing low.

4.2. Dark Count Rate

InGaAs/InP SPADs are affected by a high dark count rate due to the thermal generation of carriers [8]. We evaluated the dark count rate of the SPAD we employed when cooled down to 220 K for both gating schemes. Fig. 3(d) shows the results obtained at different excess biases (between 3 V and 7 V).

The dark count rate for the square-wave scheme has been calculated as the effective dark count rate normalized by the duty cycle (1/1000) and taking into account the Poisson statistics for multiple

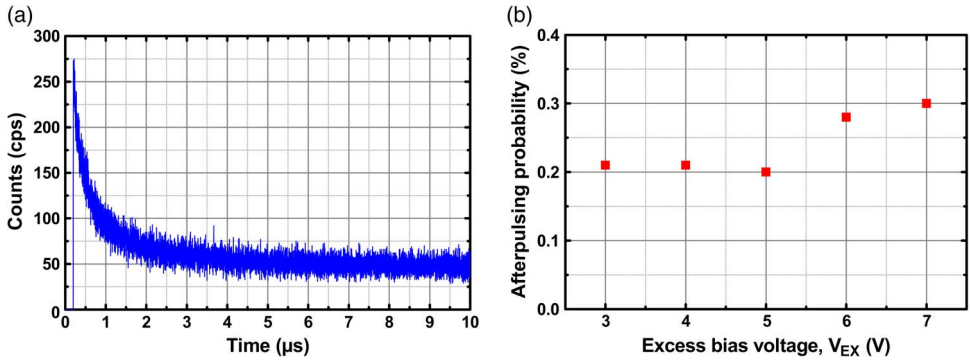

Fig. 4. Experimental measurement of gate-free InGaAs/InP SPAD afterpulsing. a) time histogram of the afterpulsing events collected by the TCCC technique with $V_{EX} = 5$ V, where the estimated time constant of carrier release is $\tau = 0.62$ μs. b) Dependence of the afterpulsing probability at different excess biases with a count-off time of 10 ns: even with $V_{EX} = 7$ V the probability is just 0.3% with the sine-wave gate-free technique.

events in the same gate window. In this way, the user has an indication of the noise level when using the device during its ON time only (e.g. with periodic signals). Instead, the dark counts for the gate-free scheme are due to the noise counts of the system without any normalization. Since the system has been developed to be used in free-running mode, this is the most direct indication of its noise level.

4.3. Afterpulsing Probability

One of the main drawbacks of InGaAs/InP SPAD is the high afterpulsing probability that usually forces the use of long hold-off times (> 1 μs) after every avalanche event when operated with the long T_{ON} square-wave approach. In fact, during each avalanche, some charge carriers flowing inside the detector get trapped by the deep-levels and are then released with a slow exponential time decay causing spurious events in the successive gates. In the typical square-wave approach, the avalanche is quenched by a combination of passive and active circuits in few nanoseconds. Therefore, too many carriers are flowing to reduce significantly the afterpulsing. With the sine gating at high frequencies (1 GHz and above) the avalanche is quenched by the gating itself, which is extremely fast (less than few hundreds of picoseconds), thus resulting in an effective strong reduction of the afterpulsing [11]–[14].

We characterized the sine-gated SPAD afterpulsing probability by means of the Time-Correlated Carrier Counting (TCCC) technique [18]. Fig. 4(a) shows the experimental data of the TCCC technique at $V_{EX} = 5$ V. The time constant of the carrier release is about $\tau = 0.62$ μs and the total afterpulsing probability is 0.1%. Fig. 4(b) reports the afterpulsing probability dependence on the excess bias voltage, showing a maximum of 0.3% at $V_{EX} = 7$ V.

Since the output comparator includes a 10 ns monostable, there is a 10 ns masking period that is necessary to avoid spurious clicks due to spikes and ringing in the avalanche signal. The count-off time also masks possible afterpulsing events in the first 10 ns after a detected avalanche event.

4.4. Timing Resolution

We measured the response of the system to a picosecond pulsed laser. We employed a pulsed laser at 1550 nm with a Full-Width at Half Maximum (FWHM) of 20 ps and a pulse repetition rate of 1 MHz. For comparison, we also performed the same measurement with a standard synchronous square-wave gating scheme.

The InGaAs/InP SPAD is operated in the following conditions when used in the sine-gated regime: gate sine wave at 915 MHz, $V_{EX} = 7$ V, count-off time $t_{count-off} = 10$ ns and temperature $T = 220$ K. The square-wave scheme, instead, is characterized by a gate repetition rate $f_{GATE} = 10$ kHz, $V_{EX} = 7$ V, $T_{ON} = 100$ ns and temperature $T = 220$ K.

Fig. 5 shows the two temporal responses: the FWHM of response for the sine-wave scheme is 150 ps (b), while the temporal response of the same device operated in conventional square-gated

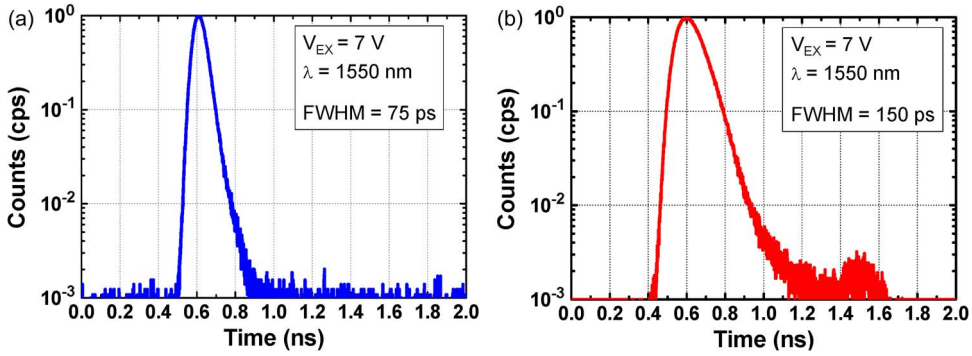

Fig. 5. Temporal responses of the InGaAs/InP SPAD to a sharp (FWHM = 20 ps) laser pulse with a repetition frequency of 1 MHz at $\lambda = 1550$ nm. a) temporal response obtained with a classical synchronous square-wave scheme (FWHM = 75 ps). b) temporal response with the sine-wave gate-free mode (FHWM = 150 ps).

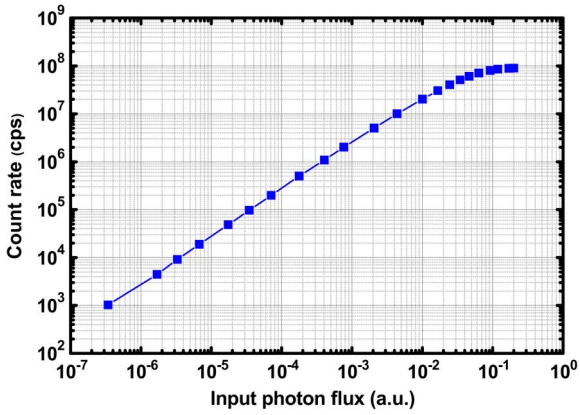

Fig. 6. Dependence of the SPAD count rate on the input photon flux for the InGaAs/InP SPAD operated in sine-wave gate-free. The linearity of the response is excellent up the saturation point at 100 Mcount/s.

mode has a FWHM of 75 ps (a). The worsening in the temporal response is due to the shape of the sine gating signal that is not flat in time: an avalanche generated with low V_{EX} (e.g. at the edges of the gate ON time) is detected after an avalanche developed with higher excess bias voltage.

In the sine-wave gate-free response [Fig. 5(b)] there is a small bump approximately 1 ns after the main peak. This bump is an artifact of the read-out circuit: the implemented 10 ns count-off time masks every signal above the comparator threshold after an avalanche has previously occurred, including afterpulsing events. Unfortunately, some avalanches are too small and are not detected by the read-out circuit but can still initiate an afterpulsing event in the successive gates, thus possibly giving above threshold pulses that are detected. Therefore, since small avalanches are not detected, no count-off is set and some afterpulsing events are present in the reconstructed waveform.

4.5. Saturated Count Rate

As described above, one of the main advantages of sinusoidal gating in the gigahertz regime is the low afterpulsing probability, even with short count-off times. With a dead time as short as $t_{count-off} = 10$ ns, the SPAD can successfully work at very high count rates, withstanding high photon fluxes. Fig. 6 shows that the detector response is linear with the input photon flux, up to the saturation reached at about $1/t_{count-off} = 100$ Mcount/s.

5. Conclusion

In this paper we presented a novel operating method for InGaAs/InP SPADs based on a gigahertz sinusoidal gate signal. By keeping the SPAD gate signal unlocked from the synchronization reference of the optical waveform to be reconstructed, a free-running equivalent mode is obtained, that we called gate-free mode.

An extensive experimental characterization has shown how the SPAD performance improves compared with a classical square-wave gating scheme, especially for non-periodic high-throughput applications. The average photon detection efficiency at 1550 nm is 3%, the afterpulsing probability with a 10 ns count-off time is below 0.3%, the timing resolution is 150 ps (FWHM) and the maximum count rate is 100 Mcount/s.

This approach is therefore a new state of the art for high throughput single-photon counting applications in the near-infrared range up to 1700 nm. Further developments will include: i) improvement of the performance by employing higher frequency sinusoidal signals with higher amplitude; ii) wider bandwidth components will allow to discriminate smaller avalanches in order to further reduce afterpulsing, increase the photon detection efficiency and increase the maximum count rate; iii) thanks to monolithic microwave integrated circuits, the system will be squeezed in a compact module for being easily deployed in real applications.

Acknowledgment

The authors would like to thank Prof. F. Zappa for support and helpful technical discussions.

References

[1] N. Gisin and R. Thew, "Quantum communication," *Nature Photon.*, vol. 1, no. 3, pp. 165–171, Mar. 2007.
[2] Q.-L. Wu, Z.-F. Han, E.-L. Miao, Y. Liu, Y.-M. Dai, and G.-C. Guo, "Synchronization of free-space quantum key distribution," *Opt. Commun.*, vol. 275, no. 2, pp. 486–490, Jul. 2007.
[3] Z. L. Yuan, J. F. Dynes, and A. J. Shields, "Resilience of gated avalanche photodiodes against bright illumination attacks in quantum cryptography," *Appl. Phys. Lett.*, vol. 98, no. 23, p. 231104, Jun. 2011.
[4] P. A. Hiskett, C. S. Parry, A. McCarthy, and G. S. Buller, "A photon-counting time-of-flight ranging technique developed for the avoidance of range ambiguity at gigahertz clock rates," *Opt. Exp.*, vol. 16, no. 18, pp. 13685–13698, Aug. 2008.
[5] N. R. Gemmell, A. McCarthy, B. Liu, M. G. Tanner, S. D. Dorenbos, V. Zwiller, M. S. Patterson, G. S. Buller, B. C. Wilson, and R. H. Hadfield, "Singlet oxygen luminescence detection with a fiber-coupled superconducting nanowire single-photon detector," *Opt. Exp.*, vol. 21, no. 4, pp. 5005–5013, Feb. 2013.
[6] G. N. Gol'tsman, O. Okunev, G. Chulkova, A. Lipatov, A. Semenov, K. Smirnov, B. Voronov, A. Dzardanov, C. Williams, and R. Sobolewski, "Picosecond superconducting single-photon optical detector," *Appl. Phys. Lett.*, vol. 79, no. 6, pp. 705–707, Aug. 2001.
[7] F. Zappa, S. Tisa, A. Tosi, and S. Cova, "Principles and features of single-photon avalanche diode arrays," *Sens. Actuators A, Phys.*, vol. 140, no. 1, pp. 103–112, Oct. 2007.
[8] M. A. Itzler, X. Jiang, M. Entwistle, K. Slomkowski, A. Tosi, F. Acerbi, F. Zappa, and S. Cova, "Advances in InGaAsP-based avalanche diode single photon detectors," *J. Modern Opt.*, vol. 58, no. 3/4, pp. 174–200, Feb. 2011.
[9] A. Tosi, A. Della Frera, A. Bahgat Shehata, and C. Scarcella, "Fully programmable single-photon detection module for InGaAs/InP single-photon avalanche diodes with clean and sub-nanosecond gating transitions," *Rev. Sci. Instrum.*, vol. 83, no. 1, p. 013104, Jan. 2012.
[10] A. Restelli, J. C. Bienfang, and A. L. Migdall, "Time-domain measurements of afterpulsing in InGaAs/InP SPAD gated with sub-nanosecond pulses," *J. Modern Opt.*, vol. 59, no. 17, pp. 1465–1471, Oct. 2012.
[11] N. Namekata, S. Adachi, and S. Inoue, "Ultra-low-noise sinusoidally gated avalanche photodiode for high-speed single-photon detection at telecommunication wavelengths," *IEEE Photon. Technol. Lett.*, vol. 22, no. 8, pp. 529–531, Apr. 2010.
[12] K. A. Patel, J. F. Dynes, A. W. Sharpe, Z. L. Yuan, R. V. Penty, and A. J. Shields, "Gigacount/second photon detection with InGaAs avalanche photodiodes," *Electron. Lett.*, vol. 48, no. 2, pp. 111–113, 2012.
[13] J. Zhang, P. Eraerds, N. Walenta, C. Barreiro, R. Thew, and H. Zbinden, "2.23 GHz gating InGaAs/InP single-photon avalanche diode for quantum key distribution," in *Proc. SPIE*, vol. 7681, *Advanced Photon Counting Techniques IV*, p. 76810Z, 2010.
[14] Y. Liang, E. Wu, X. Chen, M. Ren, Y. Jian, G. Wu, and H. Zeng, "Low-timing-jitter single-photon detection using 1-GHz sinusoidally gated InGaAs/InP avalanche photodiode," *IEEE Photon. Technol. Lett.*, vol. 23, no. 13, pp. 887–889, Jul. 2011.
[15] T. Lunghi, C. Barreiro, O. Guinnard, R. Houlmann, X. Jiang, M. A. Itzler, and H. Zbinden, "Free-running single-photon detection based on a negative feedback InGaAs APD," *J. Modern Opt.*, vol. 59, no. 17, pp. 1481–1488, Oct. 2012.
[16] J.-S. Hong, *Microstrip Filters for RF/Microwave Applications,* 2nd ed. Hoboken, NJ, USA: Wiley, 2011, p. 656.
[17] A. Tosi, F. Acerbi, M. Anti, and F. Zappa, "InGaAs/InP single-photon avalanche diode with reduced afterpulsing and sharp timing response with 30 ps tail," *IEEE J. Quantum Electron.*, vol. 48, no. 9, pp. 1227–1232, Sep. 2012.
[18] A. C. Giudice, M. Ghioni, S. Cova, and F. Zappa, "A process and deep level evaluation tool: Afterpulsing in avalanche junctions," in *Proc. 33rd Conf. ESSDERC*, 2003, pp. 347–350.